

# The spectroscopically confirmed X-ray cluster at $z = 1.62$ with a possible companion in the Subaru/XMM-Newton deep field

Masayuki Tanaka

*Institute for the Physics and Mathematics of the Universe, The University of Tokyo, 5-1-5  
Kashiwanoha, Kashiwa-shi, Chiba 277-8583, Japan*

*European Southern Observatory, Karl-Schwarzschild-Str. 2, D-85748 Garching bei München,  
Germany*

Alexis Finoguenov

*Max-Planck-Institut für extraterrestrische Physik, Giessenbachstrasse, D-8574 Garching bei  
München, Germany*

*University of Maryland, Baltimore County, 1000 Hilltop Circle, Baltimore, MD 21250, USA*

and

Yoshihiro Ueda

*Department of Astronomy, Kyoto University, Kyoto 606-8502, Japan*

## ABSTRACT

We report on a confirmed galaxy cluster at  $z = 1.62$ . We discovered two concentrations of galaxies at  $z \sim 1.6$  in the Subaru/XMM-Newton deep field based on deep multi-band photometric data. We made a near-IR spectroscopic follow-up observation of them and confirmed several massive galaxies at  $z = 1.62$ . One of the two is associated with an extended X-ray emission at  $4.5\sigma$  on a scale of  $0'.5$ , which is typical of high- $z$  clusters. The X-ray detection suggests that it is a gravitationally bound system. The other one shows a hint of an X-ray signal, but only at  $1.5\sigma$ , and we obtained only one secure redshift at  $z = 1.62$ . We are not yet sure if this is a collapsed system. The possible twins exhibit a clear red sequence at  $K < 22$  and seem to host relatively few number of faint red galaxies. Massive red galaxies are likely old galaxies – they have colors consistent with the formation redshift of  $z_f = 3$  and a spectral fit of the brightest confirmed member yields an age of  $1.8_{-0.2}^{+0.1}$  Gyr with a mass of  $2.5_{-0.1}^{+0.2} \times 10^{11} M_{\odot}$ . Our results show that it is feasible to detect clusters at  $z > 1.5$  in X-rays and also to perform detailed analysis of galaxies in them with the existing near-IR facilities on large telescopes.

*Subject headings:* galaxies: clusters: individual — galaxies: luminosity function, mass function — X-rays: galaxies: clusters

## 1. Introduction

The galaxy evolution is closely linked to the structure formation of the Universe. Isolated galaxies and those in clusters evolve in different ways and the differential evolution results in the strong environmental dependence of galaxy properties observed in the local Universe. The environmental dependence of galaxy properties is already strong at  $z = 1$ . Intensive studies of  $z \sim 1$  clusters have shown that red galaxies have already become the dominant population in clusters at  $z = 1$  (e.g., Blakeslee et al. 2003; Nakata et al. 2005; Lidman et al. 2008; Mei et al. 2009). The spectroscopically confirmed highest redshift X-ray cluster known until now is located at  $z = 1.45$  (Stanford et al. 2006), but red galaxies are abundant even in this highest- $z$  cluster (Hilton et al. 2009). A few authors reported a possible clusters at  $z > 1.5$ . For example, Kurk et al. (2009) presented an over-density of galaxies at  $z = 1.6$ , which may later collapse to a cluster. It is not detected in X-rays down to a limit of  $< 1 \times 10^{-16} \text{ergs s}^{-1} \text{cm}^{-2}$ . Andreon et al. (2009) presented a cluster at  $z_{\text{phot}} \sim 1.9$ , but its redshift has been questioned by Bielby et al. (in prep) — it is likely a complex system with one confirmed at  $z = 1.1$  and another one possibly at  $z \sim 1.5$  (see Bielby et al. for details). It is challenging to identify clusters at  $z > 1.5$ , but one has to explore this redshift regime to identify the epoch when red galaxies become the dominant population in clusters and how the environmental dependence of galaxy properties is established.

We are conducting a distant X-ray cluster survey in the Subaru/XMM-Newton Deep Field (SXDF). We refer the reader to Finoguenov et al. (2009b) for details of our survey and the construction of the deep multi-band photometric catalog<sup>1</sup>. As part of the survey, we identified two concentrations of red galaxies first by their red sequence and then we found one of the sources is also securely detected in X-rays. We estimated their redshifts to be  $z \sim 1.6$  both from the location of the cluster red sequence and from photometric redshifts. Not only they have very similar redshifts, but they are also close to each other on the sky; they are separated only by  $\sim 2.5$  arcmin ( $\sim 1.3$  Mpc at  $z = 1.6$ ). Followed by the initial photometric identification, we carried out a near-IR spectroscopic follow-up observation of the possible twin clusters and we report on the results in the paper. Recently, Papovich et al. (2010) presented a completely independent study of one of the clusters. Readers are referred to their paper for a similar, but independent analysis.

The layout of the paper is as follows. We first describe the near-infrared spectroscopic follow-up observation and present a discovery of the most distant X-ray cluster from the observation in section 2. Section 3 discusses our results and summarizes the paper. Unless otherwise stated, we adopt  $H_0 = 72 \text{km s}^{-1} \text{Mpc}^{-1}$ ,  $\Omega_M = 0.25$ , and  $\Omega_\Lambda = 0.75$ . Magnitudes are on the AB system.

---

<sup>1</sup> We note that we have revised the X-ray catalog presented in Finoguenov et al. (2009b) by adding the 0.3-0.5 keV band data from XMM. We extract the images separately using the single events, produce a corresponding background estimation, and add them to the mosaic only at the very last stage. This increases signals from distant low-mass clusters.

## 2. Observation and Discovery

We carried out near-IR multi-object spectroscopy with MOIRCS on the Subaru telescope (Ichikawa et al. 2006; Suzuki et al. 2008) on the 3rd-4th of December 2009. We selected targets for spectroscopy using photometric redshifts ; the first priority is given to red galaxies at  $1.4 < z_{phot} < 1.8$ , and second priority to blue galaxies at the same redshift range. The observing conditions were poor; 1 – 1.2 arcsec seeing in the  $J$ -band most of the time and we occasionally had clouds and high humidity. We used the  $zJ500$  grism with a slit width of 0.8 arcsec, which gave a resolving power of  $R \sim 500$ . The exposures were broken into 15 min. to 20 min. each and the total integration time amounted to 320 min. The data were reduced in a standard manner with custom-designed pipeline (Tanaka et al. 2009). The spectra were visually inspected and redshifts and confidence flags were assigned to each object. We obtained 11 secure redshifts and 5 possible redshifts out of 39 observed objects. We present sample spectra in Fig. 1.

Fig. 2 summarizes our effort. There are two distinct concentrations of red galaxies. The concentration on the top-right (SXDF-XCLJ0218-0510) is detected in X-rays at  $4.5\sigma$ , which suggests that it is a gravitationally bound system. The X-ray is extended towards West, but we suspect that this is because a gap between the pn detectors passes the Eastern part, where only MOS data contributed for the detection. It has two very bright galaxies and they have secure redshifts at  $z = 1.625$  and  $z = 1.634$ , respectively. There are two more galaxies with secure redshifts at  $z \sim 1.625$  in this system. Together with the clear concentration of the photo- $z$  selected galaxies, we are highly confident that this system is a real cluster. This is the first confirmation of a distant cluster based on near-IR spectroscopy.

Papovich et al. (2010) confirmed several low-mass blue galaxies at the same redshift, one of which is a common object at  $z = 1.649$ . Including redshifts from Papovich et al. (2010), we have 9 secure redshifts in this system, and we measure its redshift to be  $z = 1.6230^{+0.0009}_{-0.0003}$  and a velocity dispersion of  $537^{+76}_{-213}$  km s<sup>-1</sup> using the biweight estimator and gapper method, respectively (Beers et al. 1990). We note that biweight estimator gives a velocity dispersion of  $109^{+350}_{-30}$  km s<sup>-1</sup>, being consistent with the one from gapper within the errors. We take the one from gapper in the following because of its robustness against poor statistics (Beers et al. 1990). The virial mass and radius are  $M_{200} = 1.1^{+0.5}_{-0.8} \times 10^{14} M_{\odot}$  and  $R_{200} = 0.54^{+0.08}_{-0.21}$  Mpc (Carlberg et al. 1997). We note that one obtains a biased high velocity dispersion when only blue galaxies are used (Biviano et al. 2006), but half of the galaxies used here are massive red galaxies. Two galaxies at  $z = 1.642$  and  $z = 1.649$  might be background galaxies because they increase the velocity dispersion to  $1183^{+103}_{-389}$  km s<sup>-1</sup>, which seems too large, but we are not sure at this point.

The properties of the system derived from X-rays are consistent from those from optical. We detect an apparent flux of  $8.1 \pm 3.7 \times 10^{-16}$  ergs s<sup>-1</sup> cm<sup>-2</sup> at 0.5-2.0 keV (37 counts) after the point source removal (Finoguenov et al. 2009b), which can be translated into  $L_X = 3.4 \pm 1.6 \times 10^{43}$  ergs s<sup>-1</sup> at  $z = 1.6$  in the rest-frame 0.1-2.4 keV. Then, assuming the relation derived by Leauthaud et al. (2010), we obtain a cluster mass of  $M_{200} = 5.7 \pm 1.4 \times 10^{13} M_{\odot}$  and a virial radius of  $R_{200} = 0.440$

Mpc, being consistent with the optical estimates. Cluster temperature is estimated to be  $T_X = 1.7 \pm 0.3$  keV from the  $L_X - T_X$  relation as mentioned in Leauthaud et al. (2010).

We emphasize that most previous cluster studies did not remove fluxes from unresolved point sources (AGNs) once the extent of a cluster has been established. This procedure no longer works in deep surveys because the contamination from point sources is significant. We have therefore adopted the procedure in which we always remove the flux expected from detected point sources based on the shape of the PSF. In fact, we have attributed a large fraction ( $\sim 50\%$ ) of the emission around the cluster to point sources. At the XMM exposure around the cluster, if a point source contributes substantially to the overall emission ( $> 30\%$ ), it can be detected individually. We can therefore exclude a possibility of large contamination from undetected point sources to the measured extended flux. However, some of the detected point sources might be associated with the cluster core and high resolution X-ray imaging will allow us to identify potential confusions.

The one on the bottom-left (SXDF-XCLJ0218-0512) in Fig. 2 hosts an outstandingly bright galaxy, which is likely a cD galaxy of this system. We obtain a possible redshift of  $z = 1.625$  for this galaxy. Interestingly, we observe a hint of an X-ray emission right on top of the cD galaxy at  $1.5\sigma$ . Note that we do not observe nebular emission lines from the cD galaxy (see the bottom panel in Fig. 1), but we need deeper observations to confirm if the X-ray signal is real and if it is from an AGN or the cluster core. We confirm another galaxy at  $z = 1.627$  nearby. Although the concentration of galaxies around the possible cD galaxy is clear, we are not yet sure if this is a collapsed system due to the weakness of X-ray emission and to too few spectroscopic redshifts. For the rest of the paper, we assume that the two systems are real clusters at the same redshift and combine them to gain statistics. We note that our results remain unchanged if we use the secure cluster only.

### 3. Results and Discussion

The cluster red sequence is a ubiquitous feature of galaxy clusters. We draw color-magnitude diagrams in Fig. 3 using galaxies at  $< 1$  Mpc from the twins. We refer the readers to Papovich et al. (2010) for a similar analysis. The photo- $z$  selected galaxies form a clear red sequence at  $K < 22$ , while the sequence is not very clear at fainter magnitudes. We model the location of the red sequence with the updated version of the Bruzual & Charlot (2003) code, which takes into account effects of thermally pulsating AGB stars, using the procedure described in Lidman et al. (2008). Here we assume the Chabrier IMF (Chabrier 2003). A biweight fit to the red galaxies gives a sequence very close to the  $z_f = 3$  model sequence, suggesting that they are relatively old galaxies. The cosmic time between  $z = 3$  and 1.6 is 2.0 Gyr. We note that we obtain  $z_f = 3$  or higher if we use the  $z - J$  color as used in Papovich et al. (2010) who obtained  $z_f = 2.4$ . We do not know the cause of the difference in  $z_f$  at this point, but it could be due to the rather old UKIDSS catalog they used. Their paper is still under review at the time of this writing and we do not pursue this point

further. The  $z-K$  color is more sensitive to  $z_f$  at this redshift<sup>2</sup> and we prefer to use it in this paper. As a sanity check, we perform a statistical subtraction of fore-/background galaxies without using photo- $z$  following the recipe by Tanaka et al. (2005) in the right panel. A clump of red galaxies is clearly visible in the right panel as well. Again, the sequence vanishes at  $K > 22$ . There are a number of proto-clusters at even higher redshift that have a confirmed over-density of low-mass star forming galaxies (Miley & De Breuck 2008), but Fig 3 shows that a near-IR spectroscopic observation is essential to confirm the dominant population of massive galaxies in  $z > 1.5$  clusters.

To further quantify the red sequence, we plot luminosity functions (LFs) of red galaxies in Fig. 4. Here we define red galaxies as those having  $\Delta|z - K| < 0.2$  from the best fitting red sequence. We confirmed that a small change in the definition does not alter the result below. But, we should note that the current statistics is very poor. We use galaxies at  $1.4 < z_{phot} < 1.8$  and statistically subtract the remaining contamination using the entire SXDF field as a control field sample. We compare the  $z = 1.6$  LF with those at lower redshifts taken from Tanaka et al. (2008). We plot LFs relative to  $m_K^*$  at each redshift to correct for the passive evolution. The LF of the red galaxies in the twins is similar to the group LF at  $z = 1.1$ , which suggests a deficit of faint red galaxies. On the other hand, it seems that clusters at  $z = 1.6$  already host abundant massive galaxies. As seen in Fig. 3, these massive galaxies are mostly red galaxies and the clusters host few bright blue galaxies. It is hard to generalize the trend we see here with only a few clusters, but the implication would be that massive red galaxies might have become the dominant population in clusters already at  $z = 1.6$ .

Finally, we present a spectral analysis of the brightest red galaxy with secure redshift in Fig. 5. We fit the observed spectra with model spectra generated by the updated version of the Bruzual & Charlot (2003) code. We assume the exponentially decaying star formation histories and use age, dust extinction, star formation time scale, and metallicity as free parameters. We adopt the Chabrier IMF (Chabrier 2003)<sup>3</sup> and fix the redshift at  $z_{spec}$ . The fit gives an age of  $1.8_{-0.2}^{+0.1}$  Gyr and a small extinction of  $A_V = 0.2_{-0.1}^{+0.2}$  mag. Its star formation time scale is rather short,  $0.1_{-0.1}^{+0.2}$  Gyr. Assuming the exponential decay, it assembled 80% of its stars at  $z_f \sim 2.5$  that it would have at  $z = 0$ , which is in agreement with that inferred from the  $z - K$  color. Note that  $z_f = 3$  obtained from the red sequence gives an average formation redshift of the red galaxies, while we are specifically discussing the brightest red galaxy with secure redshift here. The current star formation rate is  $< 0.1M_\odot \text{ yr}^{-1}$ , which is consistent with the absence of any emission lines in the observed spectrum. Its mass is estimated to be  $2.5_{-0.1}^{+0.2} \times 10^{11}M_\odot$ , revealing the presence of such a massive galaxy in a  $z = 1.6$  cluster. As seen in lower redshift clusters, massive cluster galaxies form early and evolve passively (e.g., Thomas et al. 2005).

This study is the first result on cluster galaxies at  $z > 1.5$  using near-IR spectrograph. Our

---

<sup>2</sup> The  $z - K$  color of the model red sequence formed at  $z_f = 5$  is redder than the  $z_f = 2$  sequence by 0.74, while the difference is only 0.26 for the  $z - J$  color. Thus, the  $z - K$  color is more sensitive to  $z_f$  than  $z - J$ .

<sup>3</sup> If we use the Salpeter IMF, we obtain 1.8 times higher stellar mass. The other properties are nearly the same.

observation suggests that  $z = 1.6$  clusters exhibit a red sequence at bright magnitudes and are likely luminous in X-rays, which may have an implication for future high- $z$  cluster surveys. The cluster we discovered will evolve to a 4–5 keV cluster at  $z = 0$  (van den Bosch 2002). Such clusters are a sensitive probe of cosmology at high redshifts and yet its estimated temperature preclude a detection in a Sunyaev-Zeldovich observation. This demonstrates the power of X-ray observations in finding distant clusters. The redshift of  $z > 1.5$  is the epoch when early dark energy is important and large-scale structures at  $z > 1.5$  are a robust tracer of the primordial local non-Gaussianity (e.g., Bartelmann et al. 2006; Sadeh et al. 2007; Grossi & Springel 2009). More massive clusters than the one reported in this paper may be found in shallower X-ray observations down to  $10^{-14}$  ergs  $\text{s}^{-1} \text{cm}^{-2}$ , but one needs to survey an order of 5,000 square degrees (Finoguenov et al. 2009b), which may be difficult to follow-up photometrically. However, a similar yield in the number of clusters can be achieved by reaching  $10^{-15}$  ergs  $\text{s}^{-1} \text{cm}^{-2}$  over 100 square degrees. Therefore, deep X-ray surveys at high spatial resolution have a unique window for cosmological studies at the time when Universe was only a third of its present age. Our observation also shows that detailed analysis of galaxy populations at this redshift regime is feasible with the current near-IR facilities. This is an encouraging result and motivates us to push our X-ray cluster survey forward.

This study is based on data taken at the Subaru Telescope operated by the National Astronomical Observatory of Japan through program S09B-042. We thank Ichi Tanaka for his support during the observation. We thank the anonymous referees for their comments, which helped improve the paper.

## REFERENCES

- Andreon, S., Maughan, B., Trinchieri, G., & Kurk, J. 2009, *A&A*, 507, 147
- Beers, T. C., Flynn, K., & Gebhardt, K. 1990, *AJ*, 100, 32
- Bartelmann, M., Doran, M., & Wetterich, C. 2006, *A&A*, 454, 27
- Biviano, A., Murante, G., Borgani, S., Diaferio, A., Dolag, K., & Girardi, M. 2006, *A&A*, 456, 23
- Bruzual, G., & Charlot, S. 2003, *MNRAS*, 344, 1000
- Blakeslee, J. P., et al. 2003, *ApJ*, 596, L143
- Carlberg, R. G., Yee, H. K. C., & Ellingson, E. 1997, *ApJ*, 478, 462
- Chabrier, G. 2003, *PASP*, 115, 763
- Finoguenov, A., et al. 2009b, arXiv:0912.0039
- Grossi, M., & Springel, V. 2009, *MNRAS*, 394, 1559

- Ichikawa, T., et al. 2006, Proc. SPIE, 6269
- Hilton, M., et al. 2009, ApJ, 697, 436
- Kurk, J., et al. 2009, arXiv:0906.4489
- Leauthaud, A., et al. 2010, ApJ, 709, 97
- Lidman, C., et al. 2008, A&A, 489, 981
- Miley, G., & De Breuck, C. 2008, A&A Rev., 15, 67
- Mei, S., et al. 2009, ApJ, 690, 42
- Nakata, F., et al. 2005, MNRAS, 357, 1357
- Papovich, C., et al. 2010, arXiv:1002.3158
- Sadeh, S., Rephaeli, Y., & Silk, J. 2007, MNRAS, 380, 637
- Stanford, S. A., et al. 2006, ApJ, 646, L13
- Suzuki, R., et al. 2008, PASJ, 60, 1347
- Tanaka, M., Kodama, T., Arimoto, N., Okamura, S., Umetsu, K., Shimasaku, K., Tanaka, I., & Yamada, T. 2005, MNRAS, 362, 268
- Tanaka, M., et al. 2008, A&A, 489, 571
- Tanaka, M., Lidman, C., Bower, R. G., Demarco, R., Finoguenov, A., Kodama, T., Nakata, F., & Rosati, P. 2009, A&A, 507, 671
- Thomas, D., Maraston, C., Bender, R., & Mendes de Oliveira, C. 2005, ApJ, 621, 673
- van den Bosch, F. C. 2002, MNRAS, 331, 98

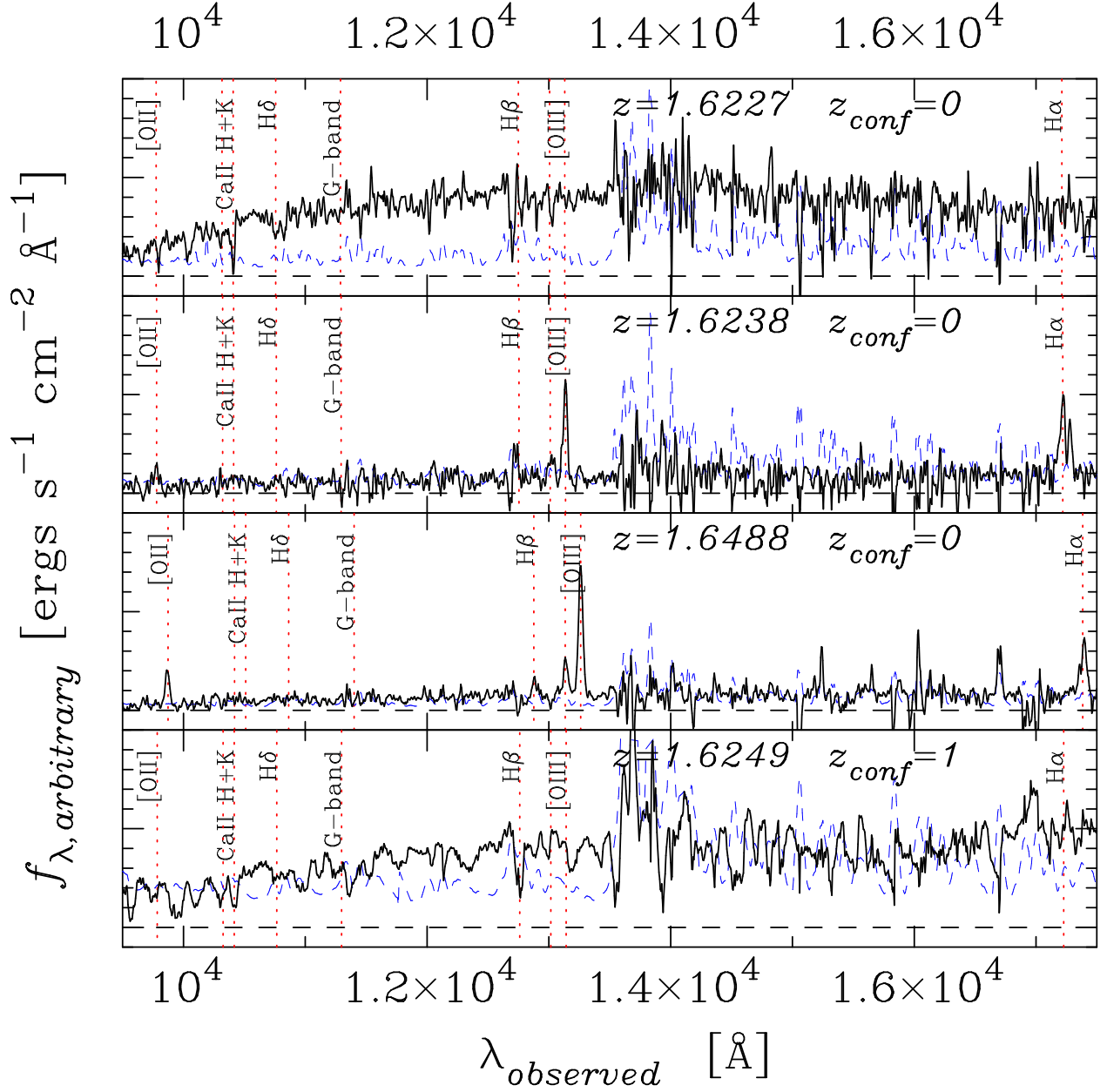


Fig. 1.— Sample spectra of  $z = 1.6$  galaxies. The dashed lines are the noise spectra. Some of the most prominent spectral features are indicated with the dotted lines.  $z_{conf} = 0$  and 1 mean secure and possible redshifts, respectively. The bottom spectrum is smoothed over 5 pixels.

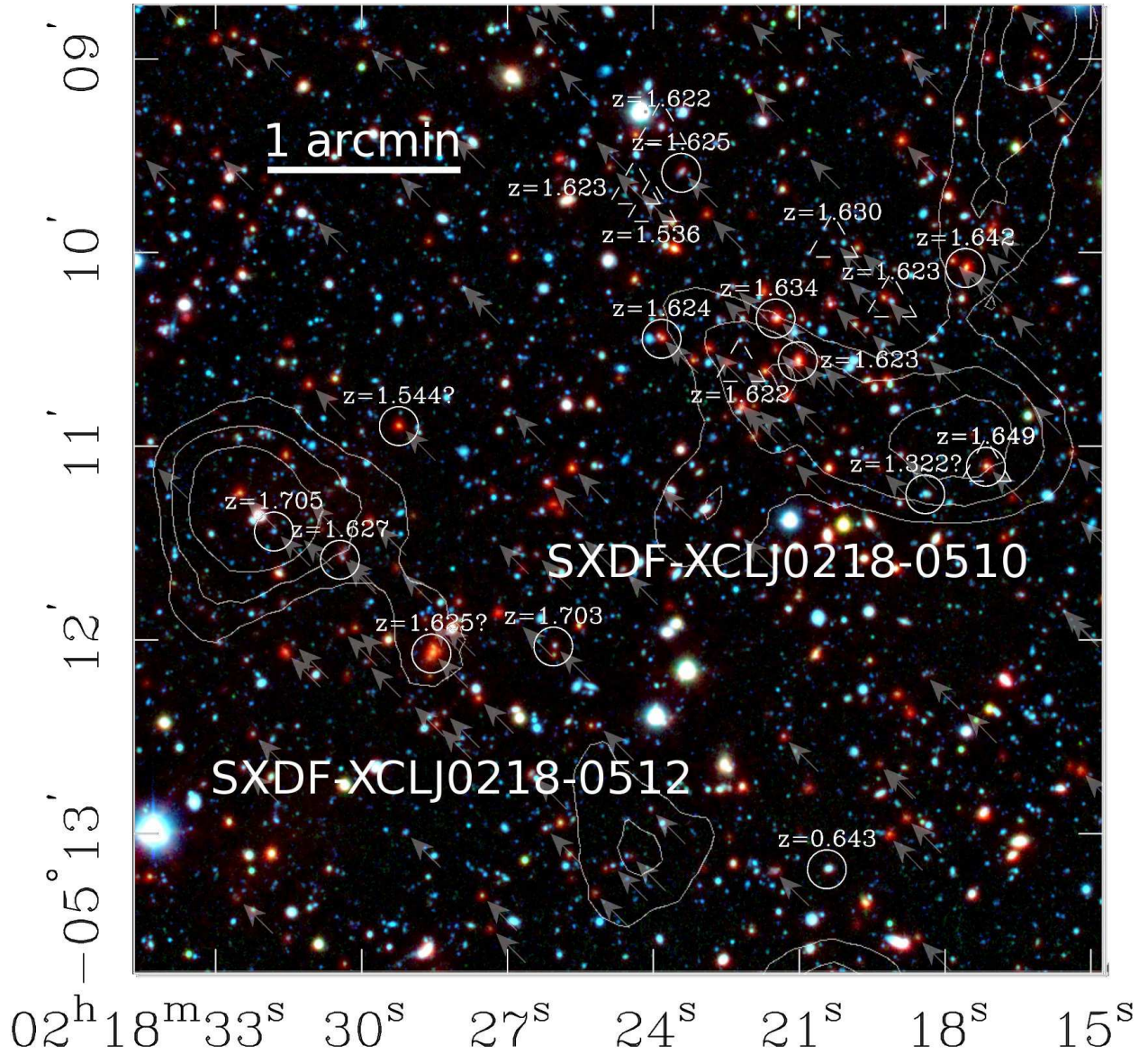


Fig. 2.—  $Rz3.6\mu\text{m}$  pseudo-color image of the twins. The image is 5 arcmin on a side. The contours show diffuse X-ray emission at the  $1.5\sigma$ ,  $3\sigma$ , and  $4.5\sigma$  levels in the 0.3–2.0 keV band and point sources are removed. The arrows indicate photo- $z$  selected potential members ( $1.4 < z_{\text{phot}} < 1.8$ ). The circles show our objects with spectroscopic redshifts and the triangles indicate spectroscopic objects from Papovich et al. (2010). The redshifts with ‘?’ are possible redshifts.

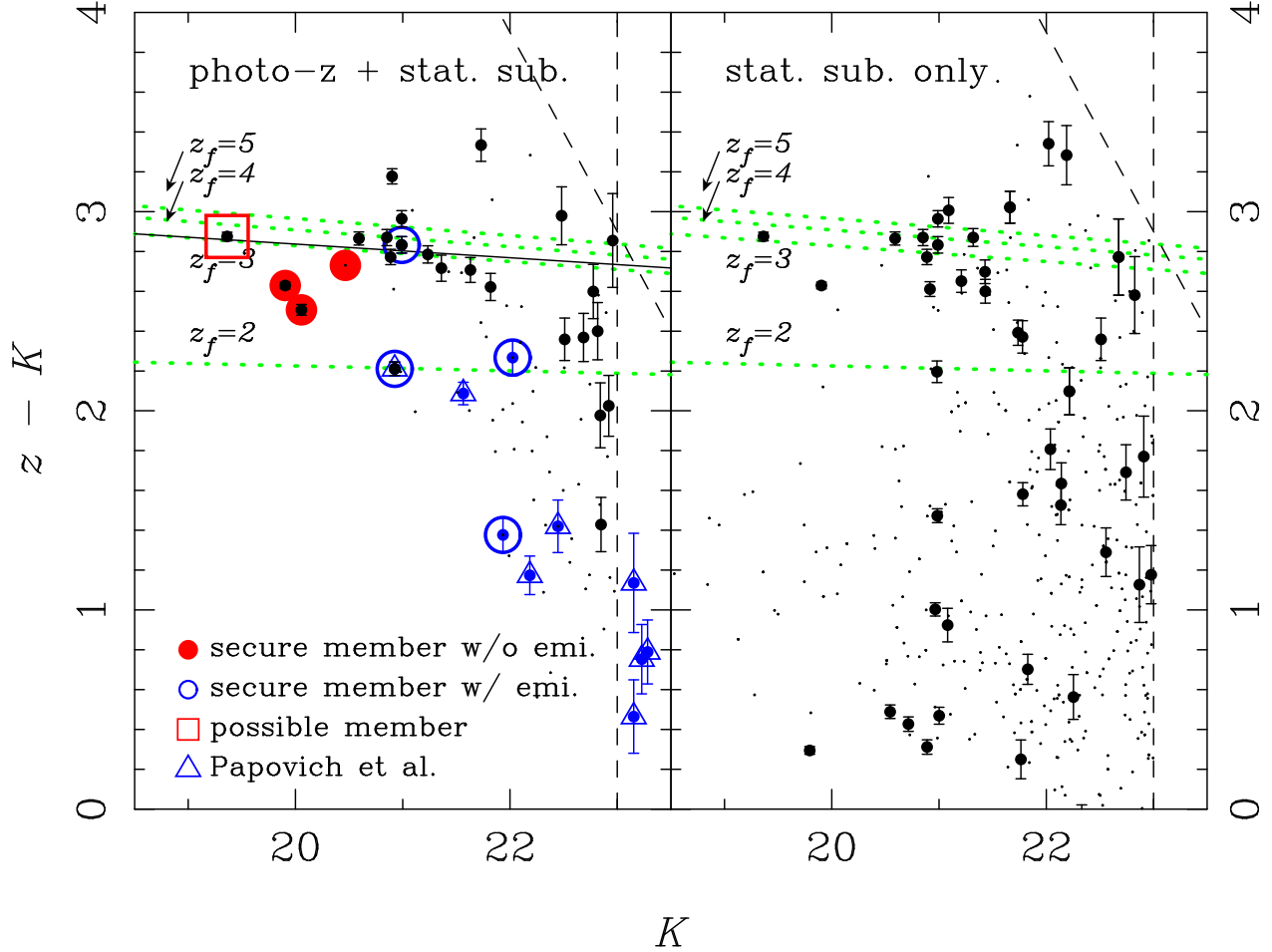


Fig. 3.—  $z - K$  plotted against  $K$ . Galaxies in the left panel are selected first by photometric redshifts ( $1.4 < z_{phot} < 1.8$ ) and then the remaining fore-/background contamination within the photo- $z$  slice is statistically subtracted. The dot and points show subtracted and remaining galaxies, respectively. We also show spectroscopic objects at  $1.62 < z_{spec} < 1.65$  and the meanings of the symbols are shown in the panel. The dashed lines show the  $K$ -band magnitude cut and  $5\sigma$  limiting colors. The dotted lines are the model red sequences formed at  $z_f = 2, 3, 4$ , and  $5$  from bottom to top. The solid line is a biweight fit to bright red galaxies ( $K < 22$  and  $z - K > 2.5$ ). We apply only the statistical field subtraction without using photo- $z$  in the right panel.

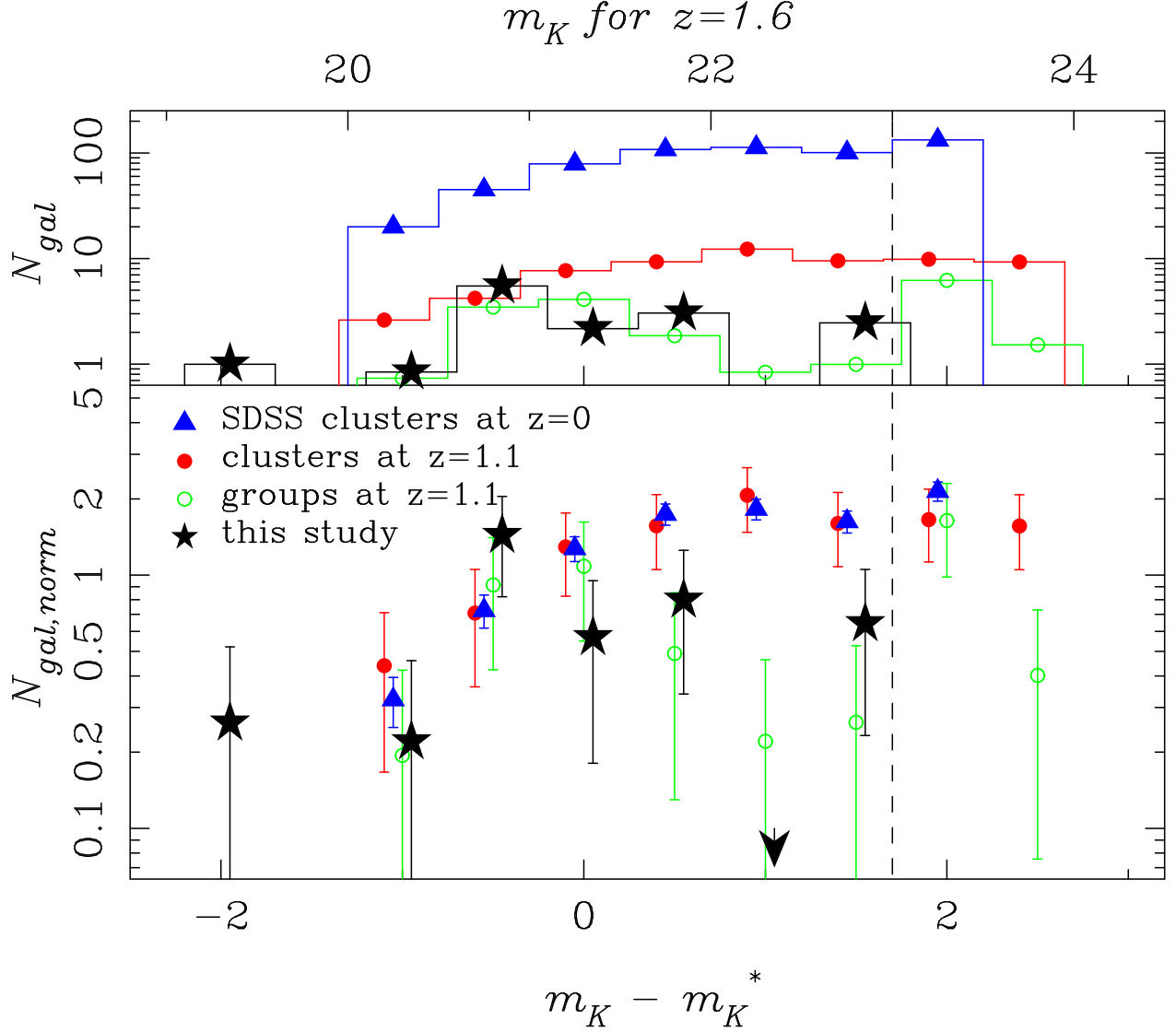


Fig. 4.— LFs of red galaxies. The top panel show the  $N_{gal}$  (after the field subtraction) and the bottom panel show  $N_{gal}$  normalized at  $\sim m_K^*$  at each redshift. The top axis shows  $K$ -band magnitudes for the  $z = 1.6$  galaxies, while the bottom axis shows  $K$ -band magnitudes relative to  $m_K^*$  at each redshift. The meanings of the symbols are shown in the plot. At  $z = 1.6$ ,  $m_K^*$  is derived by evolving  $m_K^*$  at  $z = 0$  back in time assuming  $z_f = 4$ . The points are shifted horizontally to avoid overlapping. The LFs at  $z = 0$  and  $z = 1.1$  are taken from Tanaka et al. (2008). The dashed line shows the magnitude cut of  $K = 23$  for the  $z = 1.6$  sample.

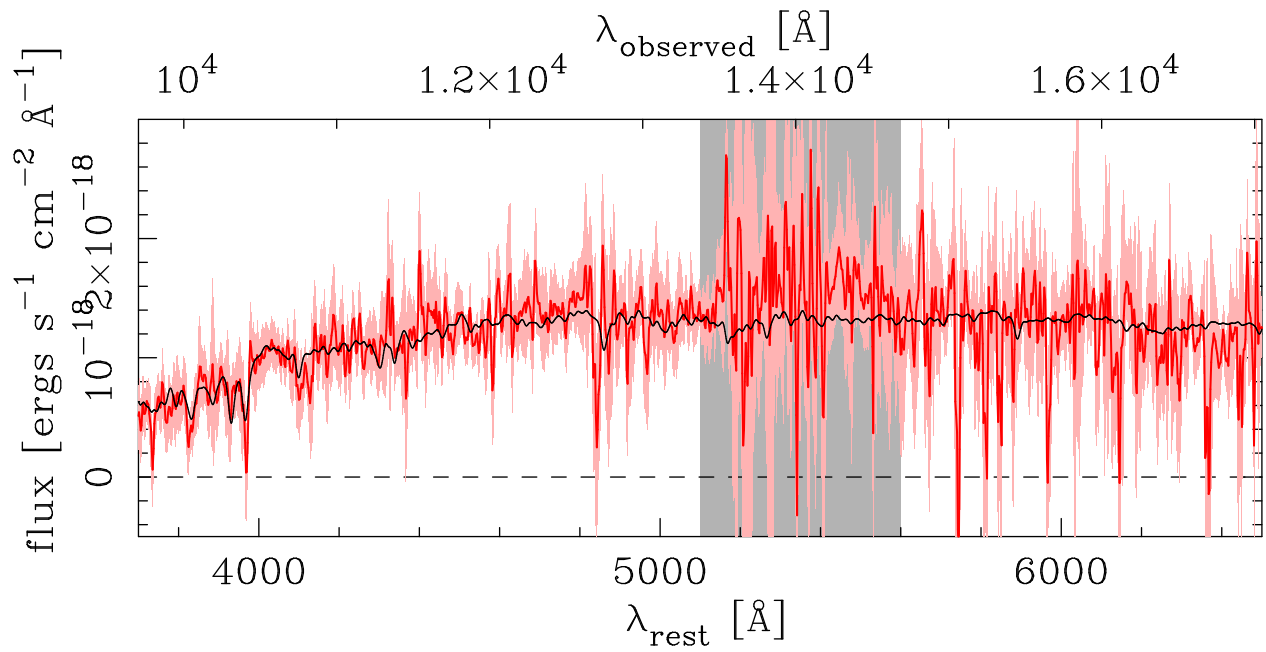


Fig. 5.— The observed spectrum of the brightest red galaxy with secure redshift (dark and light coded are the spectrum and its error) overlaid with the best-fitting model spectrum. The shaded region is not used in the fit to avoid effects of strong atmospheric extinction.